Escape of Autocrine Ligands into Extracellular Medium: Experimental Test of Theoretical Model Predictions

G. T. Oehrtman,[1] H. S. Wiley,[2] D. A. Lauffenburger[1]

[1]Department of Chemical Engineering and Center for Biomedical Engineering, Massachusetts Institute of Technology, Cambridge, Massachusetts 02139; telephone: 617-252-1629; fax: 617-252-1651; e-mail: lauffen@mit.edu
[2]Division of Cell Biology and Immunology, Department of Pathology, University of Utah Medical Center, Salt Lake City, Utah 84132

Received 03 April 1997; accepted 13 August 1997

Abstract: We have developed an experimental system for testing mathematical model predictions concerning escape of autocrine ligands into the extracellular bulk medium. This system employs anti-receptor blocking antibodies against the epidermal growth factor receptor (EGFR)/transforming growth factor alpha (TGFα) receptor/ligand pair. TGFα was expressed under the control of a tetracycline-repressed promoter, together with a constitutively expressed human EGFR in B82 mouse fibroblast cells. This expression system allowed us to vary TGFα synthesis rates over a roughly 300-fold range by adjusting tetracycline concentration. TGFα accumulation in the extracellular bulk medium was then measured as a function of cell density, TGFα synthesis rate, and anti-EGFR blocking antibody concentration. Consistent with model predictions, amounts of ligand in the medium on a per cell basis were found to diminish as cell density was increased but with reduced dependence on cell density at higher ligand synthesis rates. Similarly consistent with model predictions, higher ligand synthesis rates also decreased the effect of anti-receptor blocking antibodies. Our investigation has established that we can successfully analyze and understand autocrine ligand secretion behavior from the basis of our theoretical model. *Biotechnol Bioeng* **57:** 571–582, 1998.
Keywords: TGFα; autocrine; modeling; cell density

INTRODUCTION

Mammalian cellular functions such as differentiation, proliferation, and migration are typically regulated by interactions between growth factors and their cognate cell receptors (Sporn and Roberts, 1990). Several modes of ligand presentation to cell receptors exist, including endocrine, juxtacrine, paracrine, and autocrine. Autocrine ligand production has been found to be a common occurrence in physiological as well as pathological cellular behavior (Sporn and Roberts, 1993). Autocrine ligand/receptor ''loops'' may, in fact, enable cells to ''interrogate'' their surroundings, because interruption of autocrine ligand binding should reflect the ability of environmental components (including those on neighboring cells and those in the extracellular matrix) to interact with the ligands as they diffuse in extracellular space before rebinding to cell receptors.

A physiologically important example of a ligand/receptor system which exhibits all these characteristics (autocrine signaling, regulation of cell differentiation/proliferation/migration, interaction with extracellular matrix components) is the epidermal growth factor receptor (EGFR) and its ligand family (Gill et al., 1987; Carpenter and Wahl, 1990; Boonstra et al., 1995). EGFR is a 1186 amino acid, transmembrane glycoprotein with intrinsic protein tyrosine kinase activity. The family of currently known ligands for EGFR includes two well-characterized factors—epidermal growth factor (EGF) and transforming growth factor alpha (TGFα) (Cohen, 1962; DeLarco and Todaro, 1978), which along with others, such as amphiregulin, heparin-binding EGF, and betacellulin, can be produced by a single cell type as autocrine ligands (Barnard et al., 1994). All of the EGFR family ligands are synthesized as transmembrane proproteins, which are enzymatically cleaved on the cell plasma membrane into secreted, mature proteins; the major structural differences among them occur in an extracellular domain that may be able to interact with matrix molecules in the surrounding environment (Massague and Pandiella, 1993). These ligands have a basic 34 amino acid motif with the characteristic $CX_7CX_{4-5}CX_{10-13}CXCX_8C$ structure, where X is any noncysteine amino acid (Carpenter and Wahl, 1990). Ligand binding to EGFR initiates a cascade of biochemical processes leading to Ca^{2+} influx, protein phosphorylation, and often DNA synthesis and cell proliferation (Carraway and Cerione, 1993; Kumar et al., 1992; Gill et al., 1987). Overexpression of EGFR and/or its ligands has been found in many human carcinomas and in most squamous epithelium, hepatic, and renal carcinomas (Derynck, 1992), although it is not clear whether this overexpression is a cause or correlate of cancer.

Numerous experimental studies have aimed at determining whether anti-EGFR (''blocking'') or anti-EGF-ligand

Correspondence to: D. A. Lauffenburger

 CCC 0006-3592/98/050571-12

(''decoy'') antibodies can be effective in inhibiting growth of tumor cells possessing dysregulated autocrine loops. For instance, Van de Vijver et al. (1991) showed that EGFR tyrosine phosphorylation decreased to 30% of basal level upon addition of 20 nM monoclonal anti-EGFR antibodies in TGFα/EGFR autocrine A431 cells. Total cell EGFR mass remained constant, implying that the phosphorylation decreased as a result of blocking TGFα/EGFR binding with antibodies rather than EGFR downregulation. Modjtahedi et al. (1993a,b) obtained complete inhibition of TGFα/EGFR binding in neck and breast autocrine carcinoma cells using 100 mM rat anti-EGFR antibodies. In some other examples, addition of 30 mM anti-EGFR mAb 425 completely inhibited the proliferation of several carcinoma cell lines (Rodeck et al., 1990), whereas addition of micromolar anti-ligand antibody concentrations decreased autocrine insulin-dependent teratoma cells growth by 40% (Yamada and Serrero, 1988). Another study analyzed TGFα uptake by its receptor in Madin-Darby canine kidney cells (MDCK) transfected by basolaterally targeted TGFα expression. Dempsey and Coffey (1994) achieved a 20-fold increase in extracellular ligand levels upon addition of anti-EGFR blocking antibodies. The qualitative trends in receptor activation, ligand binding, and inhibition of cell proliferation found in these studies indicate that blocking and decoy antibodies can have a significant effect on receptor/ligand binding. However, the reasons why inhibition was or was not effectively achieved could not be elucidated for any of these cases, nor could predictions be made for other experimental conditions.

This limited ability to interpret experimental findings and to predict outcomes of future experiments arises because theoretical models have not been developed and rigorously tested, since in typical experimental studies, key system variables and parameters are not measured or controlled. As with other bioengineering systems, to understand how autocrine loops operate, and how to intervene in them, mathematical models should be helpful for determining which variables and parameters are important. As one example, mathematical modeling of the autocrine interleukin-2 (IL-2) system in T-lymphocytes has shown how multiple IL-2 receptor (IL-2R) subunits may function sequentially, providing for ligand capture and subsequent signaling (Forsten and Lauffenburger, 1994). Additionally, qualitative and quantitative effects of cell density, ligand synthesis rate, ligand/receptor binding affinity, and inhibition by anti-receptor (''blocking'') or anti-ligand (''decoy'') antibodies were predicted for IL-2 and other ligand/receptor systems (Forsten and Lauffenburger, 1992a,b). This type of theoretical analysis could be valuable for understanding how autocrine loops can be interrupted for therapeutic purposes.

Hence, to permit direct experimental testing of model predictions for autocrine systems, we have constructed an artificial TGFα/EGFR autocrine cell system in which we can control important autocrine parameters such as ligand synthesis rate and ligand/receptor binding and trafficking properties. The TGFα gene was inserted into the two-plasmid tetracycline-controlled expression system (Gossen and Bujard, 1992) and transfected into mouse B82 L fibroblasts which normally lack endogenous EGF receptors. By transfecting an EGF receptor gene into these cells we can alternatively create an autocrine ($B82R^+$/TGFα) or paracrine ($B82R^-$/TGFα) cell system. Another advantage of B82 cells is a lack of endogenously expressed ligands for the EGF receptor. Previous testing of cells transfected with EGFR show no tyrosine phosphorylation until addition of exogenous EGF (Chen et al., 1989). This autocrine EGFR/TGFα cell system was then used to test mathematical model predictions [based on the framework developed by Forsten and Lauffenburger (1994)] by measuring levels of TGFα accumulation in the extracellular bulk medium as a function of ligand synthesis rate, cell density, and concentration of anti-receptor blocking antibodies.

MATERIALS AND METHODS

General

An overview of what plasmids and how they were utilized to construct the $B82R^-$/TGFα and $B82R^+$/TGFα cell systems is shown in Fig. 1.

pUHD15.1 and pUHD10.3 from Manfred Gossen and Hermann Bujard (Gossen and Bujard, 1992), pMTE4 (transmembrane TGFα cleavable protein) from Rik Derynck (Derynck et al., 1984), the EGF receptor plasmid (pXER) and B82 mouse L cells containing pXER from Gordon Gill (Lin et al., 1986) were obtained as kind gifts. The B82 cells either lacking ($B82R^-$) or expressing human EGFR ($B82R^+$) and containing pUHD15.1 (first plasmid) were made as previously described (Will et al., 1995). The Bluescript II KS^+ plasmid was obtained from Strategene. pREP8 was purchased from Invitrogen and modified into pR8 by the removal of the EBNA-1 and OriP segments (*Sac*I to *Xba*I deletion and religation) to prevent episomal replication and allow for plasmid incorporation into chromosomal DNA.

Restriction enzymes and DNA modifying enzymes were purchased from Gibco BRL, New England Biolabs, and Boehringer Mannheim. Bovine calf serum was purchased from Hyclone. Dulbecco–Volt Modified Eagle's Media was purchased from Gibco BRL. Methotrexate, geneticin sulfate (G418), and histidinol were purchased from Sigma. Hybridomas producing monoclonal antibodies 225 and 528 were obtained from the American Type Culture Collection, and the antibodies were produced as described (Opresko et al., 1995). Both blocking anti-EGF receptor antibodies bind to EGFR with an affinity comparable to EGF and TGFα at a K_d of 2 nM (Mendelsohn et al., 1987).

B82 cells containing pUHD15.1 were selected and cultured in Dulbecco Modified Eagle's Media with 10% bovine calf serum, 1 mM glutamine, 100 units/mL penicillin, and 2.5 μg/mL streptomycin. Selection was achieved and maintained with 600 μg/mL G418. Media for the B82 cells

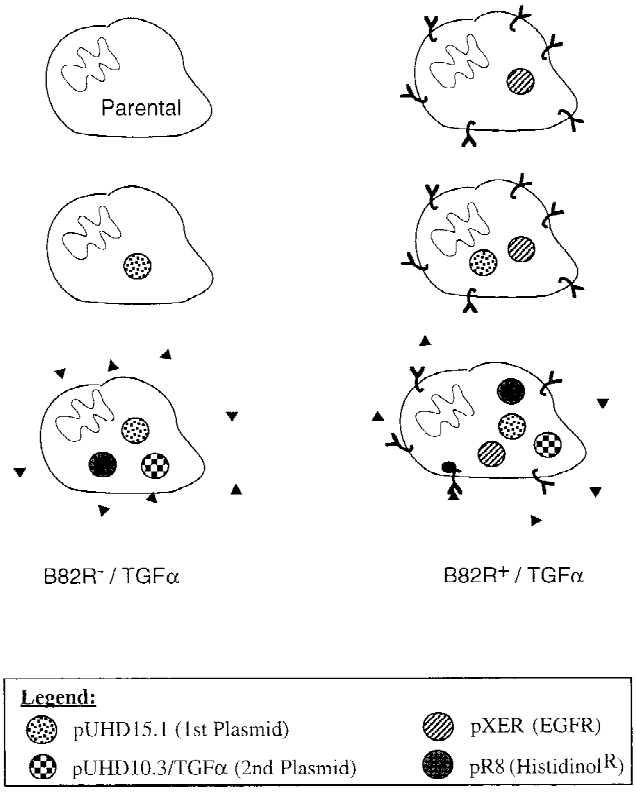

Figure 1. Artificially engineered B82 TGFα family. A schematic of plasmids required to create B82R$^-$/TGFα and B82R$^+$/TGFα cell systems. Parental cells are mouse fibroblast B82 L cells which lack endogenous expression of the EGF receptor and its ligands. Co-transfection of pUHD10.3/TGFα and pR8 (histidinol resistance) was required as pUHD10.3/TGFα lacks a resistance gene.

containing pXER (B82R$^+$) used dialyzed bovine calf serum (6,000–8,000 MWCO in PBS) and 1 μM methotrexate to maintain selection on pXER. Resistance marker on pXER is the dihydrofolate reductase (DHFR) gene which when expressed makes purines and pyrimidines. Methotrexate is an inhibitor of DHFR. Dialyzed serum is used to removed purines, pyrimidines, and thymidine and hypoxanthine. The last two are used by hypoxanthine-guanine phosphoribosyl transferase (HGPRT) to make purines and pyrimidines.

B82 cells containing pUHD15.1, pUHD10.3/TGFα and pR8 were selected and cultured in a specially defined media containing a subset of amino acids (except histidine), salts, vitamins, 10% bovine calf serum, 1 mM glutamine, 100 units/mL penicillin, and 2.5 μg/mL streptomycin. Selection was achieved and maintained with 600 μg/mL G418 and 800 μM histidinol. Suppression of TGFα secretion was achieved with 1–2 μg/mL tetracycline. Media for cells with pXER also contained dialyzed bovine calf serum and 1 μM methotrexate to maintain EGFR selection. At a later time, pR8 containing cells were switched from defined media to normal Dulbecco–Volt Modified Eagle's Media. The new media was supplemented with 10% bovine calf serum, 1 mM glutamine, 100 units/mL penicillin, 2.5 μg/mL streptomycin, 600 μg/mL G418, and 2 μg/mL of tetracycline along a histidinol increase from 800 to 2400 μM.

Construction of pUHD 10.3/TGFα

Following *Hin*dIII digestion, the 800 bp TGFα sequence was removed from pMTE4 and ligated into Strategene's Bluescript II KS$^+$ plasmid at *Hin*dIII. The TGFα insert was determined to be in pBS's T7 to T3 orientation by restriction enzyme digests. Construction of pUHD 10.3/TGFα was accomplished by cutting the TGFα sequence from pBS/TGFα plasmid with *Xho*I and *Eco*RI. pBS/TGFα was linearized with *Xho*I and blunted with Klenow enzyme, and then the TGFα insert excised by cutting with *Eco*RI. pUHD10.3 was prepared by linearizing with *Bam*HI, blunting with Klenow enzyme, and digesting with *Eco*RI. The TGFα orientation was confirmed by *Pst*I linearization and multiple enzyme digests.

Creation and Selection of Autocrine Cells

Transfection of B82 cells were accomplished using $CaPO_4$/DNA precipitation (Kriegler, 1990; Wigler et al., 1979). Briefly, a solution containing 30 μg of pUHD 10.3/TGFα and 10 μg of pR8, 450 μL of ddH_2O, 500 μL of 2× HBS (HEPES-buffered saline: 10 mM KCl, 11 mM glucose, 1.4 mM Na_2HPO_4, 171 mM NaCl, and 42 mM HEPES), and 50 μL of 2.5 M $CaCl_2$ was made. A 500 μL aliquot of pUHD10.3/TGFα and pR8 $CaPO_4$ precipitate was added to approximately 1×10^6 B82R$^+$ or B82R$^-$ cells containing pUHD15.1 (plated the previous day) in normal culture media. Media containing DNA precipitate remained on the cells for 24 h before being replaced with normal culturing media. Selection of cells incorporating pUHD10.3/TGFα was initiated 24 h later by the 1:4 dilution of cells into specially made, defined, selective media (histidinol, G418, tetracycline, and no histidine). Selective media was refreshed every third day until individual cell colonies appeared. Colonies were isolated using cloning cylinders and transferred to individual Falcon 24-well plates containing selective media.

Positive autocrine TGFα cells were determined by TGFα ELISA. Briefly, cells were plated into 3 wells of a 12-well Falcon plate (uninduced, induced, and founder cells). Upon cell confluence, cells were induced by the removal of tetracycline from the media for 24 h. On the next day, fresh media and 10 μg/mL of anti-EGFR monoclonal blocking antibody 528 was added to both uninduced and induced cells to block TGFα uptake in autocrine cells. After 24 h, conditioned media was removed and measured for TGFα content by Oncogene Science TGFα ELISA. Cell density per well was determined by Coulter Counter.

TGFα Secretion Rate

Four positive autocrine clones for expression of TGFα were tested for TGFα induction range at similar cell densities in 60 mm Corning dishes. At 24 h after plating, cells were randomly separated into two sets, and the media of one set was removed and replaced with tetracycline-free media, in-

ducing TGFα expression. The next day, all cells were rinsed and fresh 1 μg/mL tetracycline-containing or tetracycline-free media was added to their respective dishes. Cells' media also contained 10 μg/mL of anti-receptor blocking antibody 528 to prevent ligand uptake by EGFR. After a further 24 h incubation, conditioned media was removed and assayed for TGFα content by Oncogene Science TGFα ELISA kit. Cell density was determined by Coulter Counter. The TGFα secretion rate (in units of molecules/cell-minute) was then calculated by the formula: {[TGFα concentration (ng/mL) at 24 h] × [medium volume (mL)] × [6 × 10^{14} molecules/nmol]}/{[cell number] × [24 h] × [60 min/h] × [5500 ng/nmol]}.

Tetracycline Concentration Effect on TGFα Secretion

$B82R^+$ (pXER)/pUHD15.1/pUHD10.3-TGFα/pR8 autocrine clone #1 cells were plated at equal cell density in 60 mm Corning dishes and tetracycline-containing media. After 24 h, TGFα expression was induced by changing to media containing different concentrations of tetracycline from 10 to 0.001 and 0 μg/mL. The following day, the medium was replaced with medium containing the same concentration of tetracycline, but with the inclusion of 10 μg/mL of anti-receptor antibody 225. After an additional 24 h, conditioned media was removed and assayed for TGFα concentration by Oncogene Science TGFα ELISA kit. Cell density was determined by Coulter Counter.

Cellular Processing of TGFα

$B82R^-$/pUHD15.1/pUHD10.3-TGFα/pR8 cells (paracrine) were plated into twelve 100 mm Corning dishes using tetracycline-free media. The next day, the medium was removed, the cells were washed, and serum-free tetracycline-free media was added to each dish. After 6 days, all of the media was collected and concentrated using an Amicon concentrator with a YM-3 filter and using 2 mL capacity Amicon Centricon filters (3,000 MWCO) at 4°C. Media was concentrated from 60 mL down to 1 mL for a final TGFα concentration of 160 ng/mL. A total of 100 ng of TGFα was added to a mixture of protein standards which was fractionated on a 100 × 2.5 cm Sephadex G-50 fine column attached to a UV monitor and running at 40 mL/h. Fractions were collected and assayed for TGFα content using Oncogene Science TGFα ELISA kit.

Cell Density Effect

$B82R^+$ (pXER)/pUHD15.1/pUHD10.3–TGFα/pR8 autocrine clone #1 cells were serially diluted into 60 mm Corning dishes, with (0.02–1) × 10^6 cells/dish, in quadruplicate. On the next day, two sets were induced for the expression of TGFα by the removal of tetracycline from the media. Following an additional 24 h of incubation, fresh tetracycline-free or tetracycline-containing (1 μg/mL) media was added to the cells with or without mAb 225 as appropriate. Conditioned media was removed 24 h later and the TGFα concentration was determined by ELISA. Cell density per dish was determined by Coulter Counter.

RESULTS

TGFα/EGFR System Properties

An inducible TGFα expression system was made by inserting cDNA encoding TGFα into pUHD10.3. The UHD10.3 plasmid is the second plasmid of a two-plasmid, tetracycline-controlled expression system. The two-plasmid system was expressed in B82 cells that either lacked or expressed the human EGF receptor. The sequence of plasmid transfections from EGFR and TGFα negative cells to $B82R^-$/TGFα and $B82R^+$/TGFα cells is shown in Fig. 1. Seventy-two colonies were isolated, and 40 clones were successfully grown to a point suitable for testing for TGFα expression, of which 9 clones were positive (5 $B82R^+$/TGFα and 4 $B82R^-$/TGFα). The induction range of clones expressing TGFα was determined by measuring TGFα secretion rates at similar cell densities. Cells were grown in either the presence (repressed) or absence (induced) of 1 μg/mL tetracycline as well as 10 μg/mL anti-EGFR blocking antibody 528 to prevent TGFα uptake by the EGF receptor. As shown in Fig. 2, the autocrine ($B82R^+$/TGFα) clones displayed both high TGFα expression levels as well as a wide induction dynamic range. For example, the secretion rate of autocrine clone #9 increased from 0.14 to 41 ng/10^6 cells per 24 h (~10–3000 molecules/cell-minute) upon removal of tetracycline, roughly a 300-fold increase. The second highest expressor, autocrine clone #1, displayed a roughly 25-fold induction (from 1.5 to 36 ng/10^6 cells per

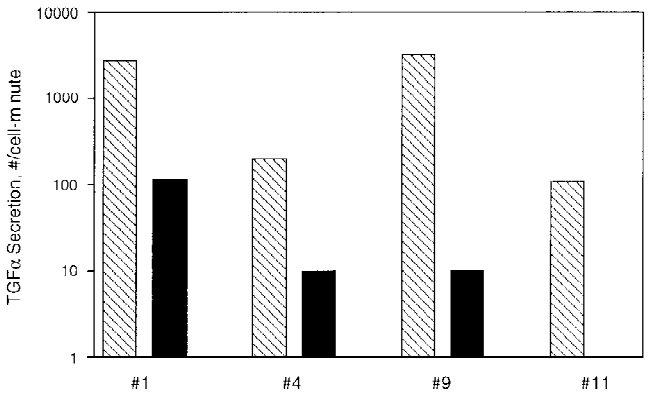

Figure 2. EGFR/TGFα expression at similar cell density. Induced TGFα expression by removal of tetracycline shown as striped. Uninduced TGFα expression repressed by 1 μg/mL tetracycline in media shown as solid. Half of the plated cells were pre-induced for the expression of TGFα by removal of tetracycline from the media. The following day, tetracycline-containing and tetracycline-free media were added to the appropriate wells and TGFα concentrations were allowed to accumulate for 24 h. In addition, media contained 10 μg/mL monoclonal antibody 528 to prevent ligand uptake by EGFR. Cell density was determined at the end of the experiment to average around 900,000 cells/60 mm dish.

24 h (~100–2700 molecules/cell-minute). Ten μg/mL (50 nM) of blocking antibody has been shown to be a sufficient concentration to prevent TGFα uptake by EGFR (Dempsey and Coffey, 1994).

An advantage of the tetracycline-controlled two-plasmid system is the ability to adjust protein expression by varying tetracycline concentrations. As shown in Fig. 3, reduction in tetracycline concentrations resulted in a stepwise increase in TGFα production rates. The induction range observed for autocrine clone #1 was over 80-fold, similar to the results shown in Fig. 2. A tetracycline concentration of 1 μg/mL appeared optimal for inhibiting TGFα production and will be the concentration used in the remaining experiments for uninduced cells.

The TGFα expression vector encodes the full-length, transmembrane form of the TGFα precursor. To ensure that the expressed protein was correctly processed into the mature 5.5 kDa form, conditioned medium from a paracrine clone was analyzed by gel filtration. As shown in Figure 4, TGFα eluted from the column at a position near the 6.5 kDa protein standard. This indicates that TGFα produced by the B82 cells is correctly processed from the 25 kDa transmembrane precursor into the mature 5.5 kDa protein.

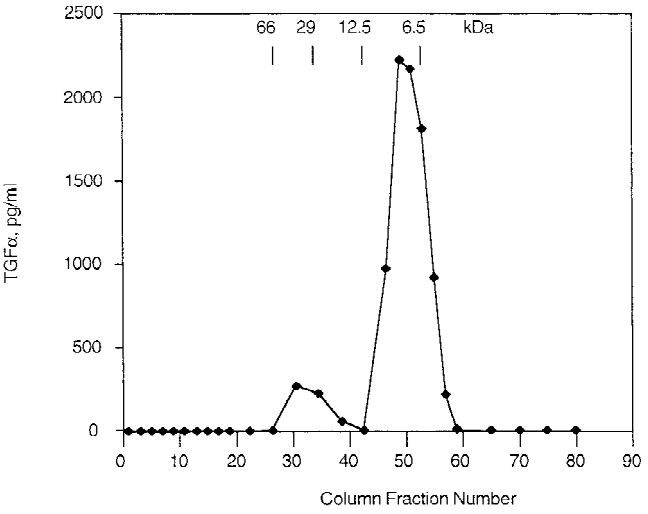

Figure 4. Determination of TGFα's molecular weight in conditioned media using a G-50 Sephadex column. Conditioned media from B82R$^-$/TGFα cells were concentrated using Amicon filters before adding to a 100 × 2.5 cm G-50 Sephadex column. Appropriate molecular standards were run simultaneously with the conditioned media. Fractions were collected every 5 min and measured at $A_{280\ nm}$ for total protein and TGFα ELISA.

Mathematical Model Predictions

Mathematical modeling work has been applied previously to the IL-2 autocrine system for T-lymphocytes, which are anchorage-independent cells that grow in suspension (Forsten and Lauffenburger, 1992a,b, 1994). However, our B82 cell TGFα/EGFR autocrine system is anchorage-dependent. Therefore, we modified the existing model from an anchorage-independent to -dependent cell situation. Figure 5A is a schematic illustration of the suspended cell situation from Forsten and Lauffenburger (1992a) showing important variables and parameters; the model equations are listed in Table I. Appendix A contains the initial starting conditions for the model along with nomenclature, parameter values, and references. Figure 5B is a schematic of the anchorage-dependent cell situation showing additional relevant parameters. The secretion layer as determined from the analysis by Berg (1983) remains the same between the suspension and anchored model. However, anchored cells have an advantage over suspended cells in that they are closer together in a 2D environment versus 3D environment. This close proximity of cells and cell–cell interactions suggests an intermediate boundary layer between the anchorage substratum and the bulk medium, represented by an intermediate volume parameter, V_i. Computer simulations with varying volume heights shows little effect on ligand concentrations and selected to be 25 μm (Forsten and Lauffenburger, 1992a). Thus, bulk volume, V_B, is the total volume minus cell, secretion, and intermediate layer volumes. As all calculations are based on volume per cell, the bulk volume and intermediate volumes need to be determined on a cell basis. Ψ, the cell area (cm^2/cell), is a parameter based on assuming an evenly dispersed cell population on a defined surface area. V_i is calculated as intermediate boundary height times Ψ, minus cell and secretion layer volumes. V_B is equal to Ψ times the difference in media height and intermediate boundary layer height in a culture dish. Extra diffusion terms are required for ligand and antibody trafficking between the intermediate boundary layer, secretion layer, and

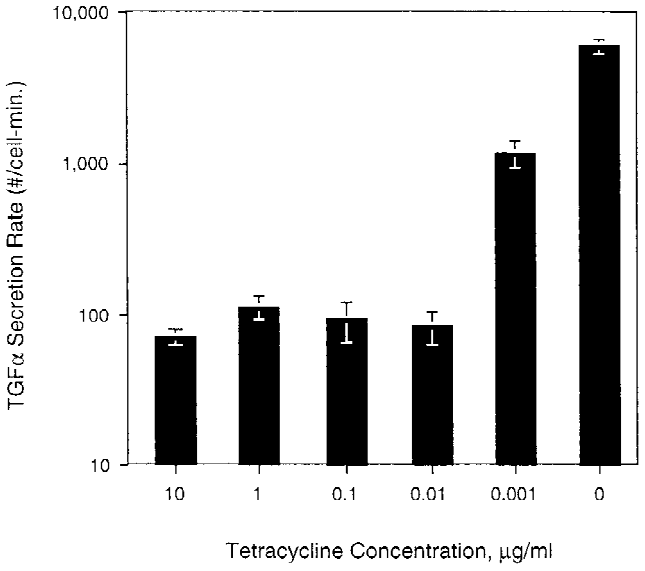

Figure 3. Tetracycline-controlled TGFα expression. Plated B82R$^+$/TGFα clone #1 cells were pre-induced for the expression of TGFα by addition of fresh media containing the tetracycline gradient for 24 h. The next day, fresh media containing the tetracycline gradient was placed on the cells and TGFα concentration allowed to accumulate for 24 h. A 10 μg/ml concentration of monoclonal antibody 225 was added to each well to prevent ligand uptake by EGFR. Cell density was determined at the end of the experiment to average around 2 million cells/60 mm dish.

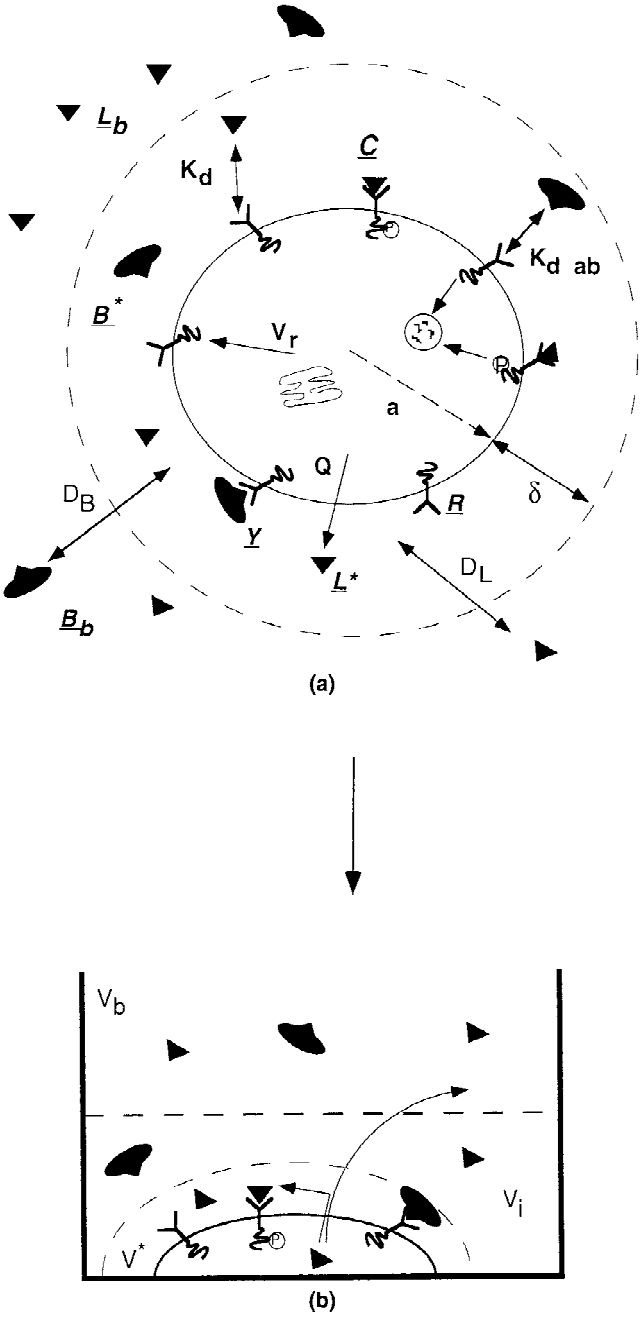

Figure 5. Autocrine computer models with blocker antibodies. Important parameters are denoted in plain text, important variables are denoted in italics and underlined. (A) Suspended autocrine cell schematic (adapted from Forsten and Lauffenburger, 1992b). (B) Anchorage-dependent autocrine cell schematic.

bulk volumes. Thus, the following terms were included in Eqs. (6), (7), (5), and (3), respectively, of Table I:

$$-\Delta^{i}_{L}(L_B - L_i), \tag{1a}$$

$$-\Delta^{i}_{B}(B_B - B_i), \tag{1b}$$

$$-\Delta^{*}_{L}(L_i - L^*), \tag{1c}$$

$$-\Delta^{*}_{B}(B_i - B^*), \tag{1d}$$

where

$$\Delta^{i}_{L} = (\pi D_L \Psi^2)/\delta_{int}, \tag{2a}$$

$$\Delta^{i}_{B} = (\pi D_B \Psi^2)/\delta_{int}, \tag{2b}$$

$$\Delta^{*}_{L} = 2\pi D_L (a + \delta), \tag{2c}$$

$$\Delta^{*}_{B} = 2\pi D_B (a + \delta). \tag{2d}$$

Figure 6 shows model predictions of occupied receptors fraction (cell receptor/ligand complex numbers divided by initial receptor number) as a function of anti-receptor blocking antibody concentration and ligand secretion rates for plated cells. Four ligand secretion rates were chosen, two of which correspond to the induced secretion rates of autocrine clone #1 measured during the cell density experiment discussed later. The experimental ligand secretion rates are 30 molecules/cell-minute (uninduced expression) and 6200 molecules/cell-minute (induced expression). Other parameter values are given in the figure legend. Note that the receptor/ligand complex level are low compared to the total number of receptors available. However, Knauer et al. (1984) showed that only a small proportion of the total steady state receptors are required to initiate a mitogenic response, at least in fibroblasts. We are currently developing a quantitative methodology to measure cell receptor/ligand complex numbers in autocrine cells (Oehrtman et al., 1997), but for an initial test of model predictions we focus here on autocrine production, i.e., the amount of ligand that escapes cell receptor binding and accumulates in the extracellular bulk medium. A key qualitative prediction from the model is that blocking antibody concentrations must be at least 1 nM (0.2 μg/mL) to reduce the number of cell surface ligand/receptor complexes to essentially zero and prevent receptor ligand uptake.

Predictions for the amount of bulk ligand on a per cell basis are plotted as a function of cell density in Fig. 7A, for ligand synthesis rates of 30 and 6200 molecules/cell-minute and other parameter values given in the figure legend. One prediction is that at low cell densities, the per-cell ligand levels should be similar regardless of the presence of blocking antibodies, but as cell density is increased the per-cell ligand levels decrease in the absence of antibody. This ''clearance'' is due to endocytic degradation mediated by binding to cell receptors (Will et al., 1995). Upon addition of blocking antibodies (at a concentration of 20 μg/mL, or

Table I. Autocrine blocking antibody model equations.

1. $dR/dt = -k_t R + V_r - k_{on} L^* R + k_{off} C - k^{B}_{on} B^* R + k^{B}_{off} Y$
2. $dC/dt = k_{on} L^* R - k_{off} C - k_e C$
3. $V^* \, dB^*/dt = -k^{B}_{on} B^* R + k^{B}_{off} Y + \Delta^{*}_{B}(B_i - B^*)$
4. $dY/dt = k^{B}_{on} B^* R - k^{B}_{off} Y - k_1 Y$
5. $V^* \, dL/dt = -k_{on} L^* R + k^{B}_{off} C + \Delta^{*}_{L}(L_i - L^*) + Q$
6. $V_B \, dL_B/dt = -\Delta^{i}_{L}(L_B - L_i)$
7. $V_B \, dB_B/dt = -\Delta^{i}_{B}(B_B - B_i)$
8. $V_i \, dL_i/dt = -\Delta^{*}_{L}(L_i - L^*) + \Delta^{i}_{L}(L_B - L_i)$
9. $V_i \, dB_i/dt = -\Delta^{*}_{B}(B_i - B^*) + \Delta^{i}_{B}(B_B - B_i)$

Note. $\Delta^{*}_{L} = 2\pi D_L (a + \delta)$; $\Delta^{*}_{B} = 2\pi D_B (a + \delta)$; $\Delta^{i}_{L} = \pi D_L \Psi^2/\delta_{int}$; $\Delta^{i}_{B} = \pi D_B \Psi^2/\delta_{int}$.

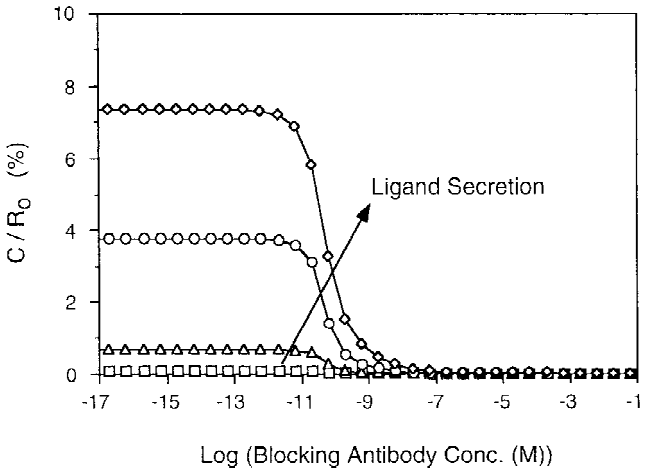

Figure 6. Fraction of occupied receptor model predictions. Anchorage-dependent autocrine cell model predictions of receptor/ligand complex levels as function of blocking antibody concentration and ligand secretion rate. Ligand secretion rates are 30 (squares), 300 (triangles), 2,000 (circles), and 6,200 (diamonds) molecules/cell-minute. Starting conditions are no ligand secretion, no receptor–antibody complexes, all receptor on cell surface and antibody present. Cell density = 1×10^5 cells/plate, k_t = 0.03 min^{-1}, k_{on} = 1.2 × 10–13 cm^3/site-min, k_{off} = 0.34 min^{-1}, $a = 5 \times 10^{-4}$ cm, $\delta = 5 \times 10^{-6}$ cm, $\delta_{int} = 25 \times 10^{-4}$ cm, R_o = 100,000 receptors/cell, $D_L = 9 \times 10^{-5}$ cm^2/min, $D_B = 2 \times 10^{-5}$ cm^2/min, dish radius = 3 cm, media = 5 cm^3, antibody k_{on} and k_{off} same as ligand k_{on} and k_{off}, time = 24 h.

approximately 100 nM), ligand levels increase compared to cells without antibody. In the presence of blocking antibody, receptor-mediated ligand uptake is inhibited and extracellular bulk ligand concentrations remain constant regardless of cell density. A second observation is a predicted difference in ligand clearance between low and high synthesis rates. At a low synthesis rate, the ligand is rapidly lost from the media at high cell densities. At a high ligand synthesis rate, ligand levels begin to decrease at the same cell density, but less significantly at higher cell densities when compared to the low ligand secreting cells in the absence of antibody. This difference is due to competing rates of ligand synthesis and receptor-mediated ligand degradation. At the higher ligand secretion rates, autocrine cells are simply creating more ligand than they can take up, becoming ''pseudo-paracrine'' cells (Will et al., 1995).

A common method of analyzing bulk ligand concentrations is to plot total ligand concentration per plate as shown in Fig. 7B. Using this analysis, ligand accumulation increases linearly with increasing cell population in both the presence and absence of blocking antibodies at high ligand secretion rates. At lower secretion rates, ligand accumulation is also linear in the presence of antibody, due to the prevention of receptor-mediated ligand uptake and reaches an equilibrium between ligand uptake and secretion in the absence of antibody. Both methods are valid, allowing the experimenter to analyze and interpret the data two different ways: ligand equilibrium versus reduced ligand levels per cell.

Confirmation of these theoretical predictions is found in the experimental data shown in Fig. 8A and 8B. Induced

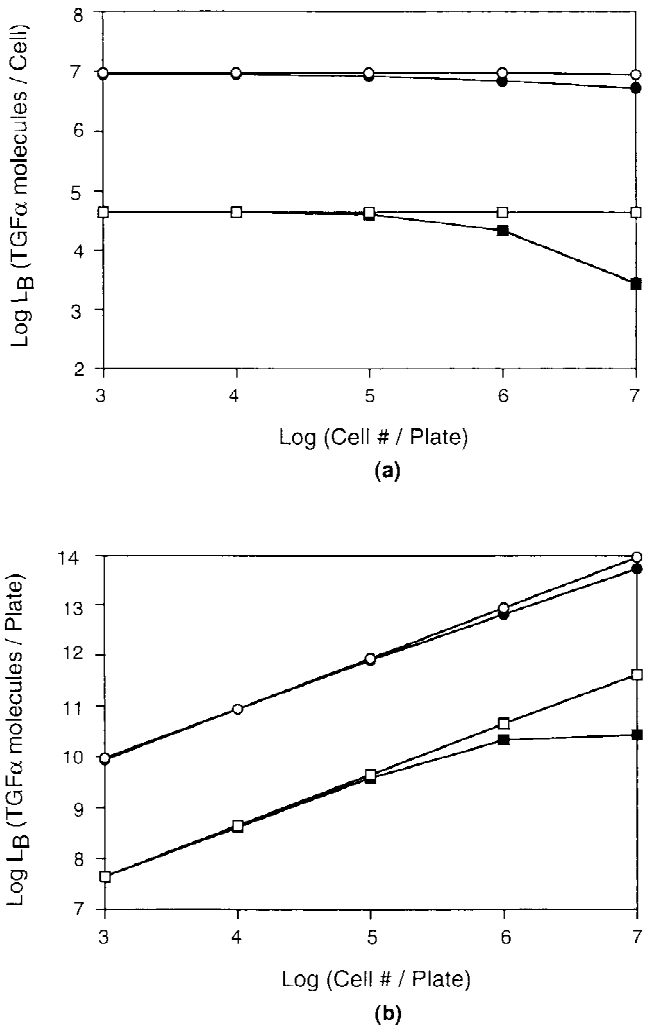

Figure 7. Bulk ligand concentration model predictions. Anchorage-dependent autocrine cell model predictions of extracellular ligand concentration as a function of cell density, ligand secretion rates, and blocking antibody concentrations. Ligand secretion rates are 30 (squares) and 6,200 (circles) molecules/cell-minute. (A) Bulk ligand concentration as TGFα molecules/cell. (B) Bulk ligand concentration as TGFα molecules/plate. Antibody concentrations are 0 {−17M Log} (solid) and 20 {−6.7M Log} (open) μg/mL. k_t = 0.03 min^{-1}, k_e = 0.3 min^{-1}, $k_{on} = 1.2 \times 10^{-13}$ cm^3/site · min, k_{off} = 0.34 min^{-1}, $a = 5 \times 10^{-4}$ cm, $\delta = 5 \times 10^{-6}$ cm, $\delta_{int} = 25 \times 10^{-4}$ cm, R_o = 100,000 receptors/cell, $D_L = 9 \times 10^{-5}$ cm^2/min, $D_B = 2 \times 10^{-5}$ cm^2/min, dish radius = 3 cm, media = 5 cm^3, antibody k_{on} and k_{off} same as ligand k_{on} and k_{off}, time = 24 h.

and uninduced TGFα expression was measured in autocrine clone #1 as a function of competing antibodies and cell density. The induction range in this experiment was 200-fold, going from 30 to 6200 molecules/cell-minute upon removal of tetracycline. At each cell density, half of the dishes received 20 μg/mL anti-EGFR blocking antibody 225 to determine whether the inhibition of TGFα uptake would vary as a function of cell density. As shown in Fig. 8A, at a high ligand synthesis rate of ~6200 molecules/cell-minute, TGFα levels were not increased by the addition of blocking antibodies. This data are in contrast with those obtained at the low synthesis rate of ~30 molecules/cell-minute for uninduced cells. In this case, TGFα levels drop

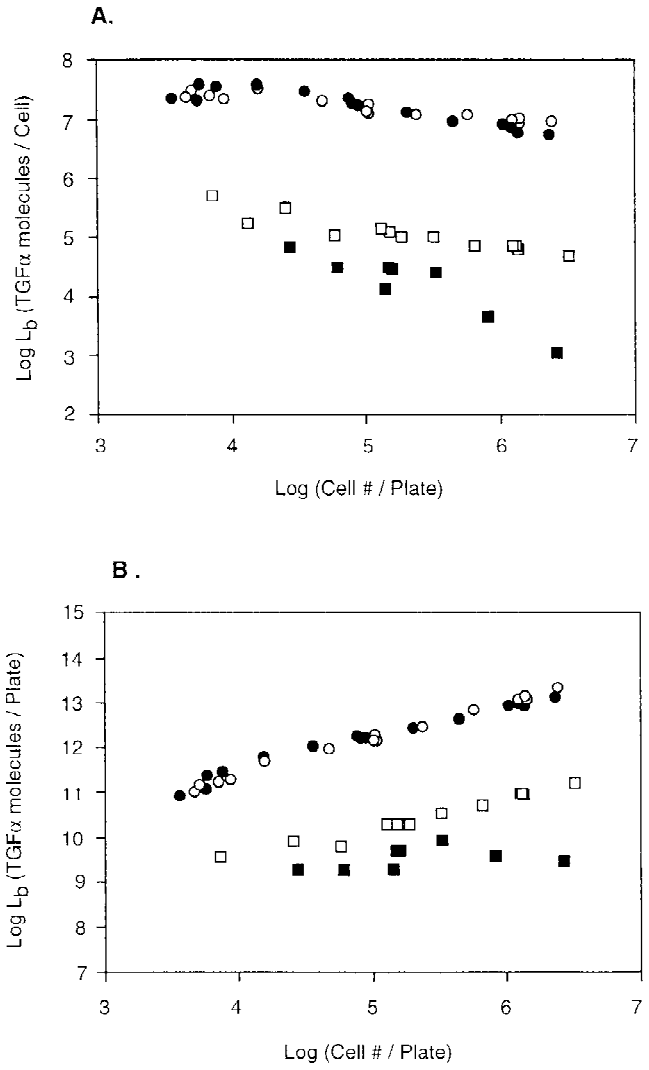

Figure 8. Experimental bulk ligand concentration. B82R$^+$/TGFα clones #1 induced (circles) and uninduced (squares) ligand concentrations were tested as a function of cell density and ligand expression levels. TGFα expression occurred with 20 μg/mL anti-EGFR monoclonal antibody 225 (open) and without antibody (solid). Half of the cells were pre-induced for the expression of TGFα by the removal of tetracycline 24 h before beginning the experiment. The following day, cells received mAb225 or not in fresh tetracycline-free or tetracycline-containing (1 μg/mL) media as appropriate, giving four experimental conditions. TGFα was allowed to accumulate in the media for 24 h before measuring ligand concentration by TGFα ELISA. (A) Bulk ligand concentration as TGFα molecules/cell. (B) Bulk ligand concentration as TGFα molecules/plate.

sharply to background levels in the absence of blocking antibody. Upon addition of EGFR blocking antibody, TGFα uptake is reduced, reaching an equilibrium. Figure 8B is plotted as total bulk ligand concentrations. As in Fig. 7B, ligand accumulation increases with increasing cell populations in the presence of antibody at the higher ligand secretion rate. Upon removal of the antibody, significant ligand accumulation does not occur for low ligand secreting cells, similar to Fig. 7B. Thus, our experimental findings are both qualitatively and quantitatively consistent with our model predictions that the effectiveness of receptor-blocking antibodies is strongly dependent on both cell density and ligand synthesis rate.

DISCUSSION

The aim of this present study was to develop a TGFα/EGFR autocrine system suitable for testing mathematical model predictions, arising from our global objective of developing a capability for understanding and predicting autocrine loop behavior. To achieve this aim, we have placed the TGFα gene under control of an inducible, high expression two-plasmid system that would allow a wide range of TGFα synthesis rates to be investigated. Indeed, we found that a progressive decrease in tetracycline levels could result in up to a 300-fold increase in TGFα production. The secretion values we obtained, approximately 3,000–6,000 molecules/cell-minute, are in the same range as several common carcinomas and cell lines (Table II). Note, however, that most of the investigators did not use anti-receptor (''blocking'') antibodies to obtain a ''true'' secretion rate by preventing ligand uptake as proven important in Figs. 7 and 8. Another piece of information typically missing in the literature is the cell density and plate size, i.e., 100,000 cells in a 96-well plate versus 100-mm dish. This inducible TGFα expression system was transfected in cells either lacking or possessing human EGFR, thus allowing us to directly compare paracrine to autocrine ligand production. In addition, because of the availability of monoclonal antibodies that block ligand binding to the EGFR, the effective number of ligand binding sites per cell could be easily changed. Because many of the quantitative parameters of our artificial autocrine system could be selectively modified, it allowed us to compare experimental data with theoretical model predictions.

In the past, investigations into autocrine signaling have been restricted to particular autocrine cell lines with given ligand synthesis rates, receptor numbers, ligand/receptor binding affinities, and ligand/receptor trafficking parameters. In some cases, random variations of one or two parameters could be obtained by cellular adaptation to modi-

Table II. Comparison of autocrine TGFα/EGFR cells.

Cell type	Secretion rate (ng/million cells · day)	Reference
Autocrine clone #1	1–40	
A431	10[a]	Reiss et al., 1991
MDA468	50	Hamburger and Pinnamaneni, 1992
MCF-7	5.2	Fontana et al., 1992
Ishikawa	2.4	Gong et al., 1992
MDCK/TGFα 1–16	0.4[b]	Dempsey and Coffey, 1994

Note. Referenced cells (except Dempsey and Coffey) did not use blocking antibodies to prevent ligand uptake by the receptor. [a]TGFα concentration given as ng/mL, assuming a 10 mL volume. [b]Assuming cell doubling every day from initial cell density given.

fied or additive media components (e.g., Filmus et al., 1987). The system we describe here overcomes many of the limitations in experimental analysis of autocrine loop behavior because most system parameters can be varied in a systematic manner. TGFα is synthesized as a transmembrane protein and enzymatic cleaved into the media where it can bind its EGF receptor. Once bound, the receptor–ligand complex initiates receptor signalling via the secondary signaling pathway, leading to cell proliferation and migration. Also upon receptor/ligand binding, the complex is internalized and processed via recycling or degradation pathways. All of the above trafficking events can potentially be manipulated in our autocrine system by mutating the ligand and/or receptor with a resulting change in receptor binding, internalization and trafficking. In addition to the autocrine TGFα/EGFR system described in this paper and the previously reported EGF/EGFR system (Will et al., 1995), we have created several other autocrine EGF cells coexpressing mutated EGF receptors (Table III).

Our global objective, as stated above, is to develop conceptual insights concerning autocrine system operation by developing theoretical models capable of predicting effects of key system parameters. Here we have predicted and experimentally tested effects of three key parameters—cell density, ligand secretion rate, and absence vs presence of blocking antibodies—on the central system variable, extracellular bulk medium ligand level. Experimental tests of effects of these same parameters on the other central system variable, cell receptor/ligand complex number, are the subject of ongoing work in our laboratory.

As shown in Figs. 7 and 8, our theoretical model predictions and experimental measurements exhibit quite similar trends. As cell density increases, ligand levels on a per-cell basis decrease once a threshold cell density is obtained in the absence of antibody (Figs. 7A and 8A). At low ligand secretion rates, ligand levels decrease past this same threshold cell density even on a bulk concentration basis (Figs. 7B and 8B). A qualitatively similar effect has been previously observed for autocrine TGFα secreted by a colon carcinoma cell line (Zorbas and Yeoman, 1993). This ligand loss is due to receptor-mediated endocytic uptake degradation (Will et al., 1995), which can reversed to some extent by the addition of blocking antibodies but only at low ligand secretion rates. The finding that blocking antibodies influence bulk medium ligand concentrations only at low ligand secretion rates indicates that at high ligand secretion rates the cells are operating essentially in paracrine rather than in purely autocrine mode. The level of ligand secretion rate at which this switch from autocrine to paracrine operation occurs is essentially equal to the receptor synthesis rate (Will et al., 1995), demonstrating the capability of cells to control autocrine loop operation in different ways.

Despite the excellent agreement between our theoretical model predictions and our experimental data, it must be noted that a number of our model assumptions may not be entirely valid. Mainly, the model parameters are considered here as constants, while it is known that some of them show dependence on system variables. For instance, the receptor/ligand complex internalization rate constant, k_e, has been shown to vary with the number of cell surface complexes (Lund et al., 1990), the receptor synthesis rate may vary in response to ligand/receptor binding (Earp et al., 1986), and the ligand synthesis rate may also vary in response to ligand/receptor binding (Barnard et al., 1994). Also, the degree of ligand and receptor recycling may be nonzero, depending on the number of intracellular complexes as well as the ligand type (French et al., 1994).

Our results underscore the necessity for measuring bulk ligand concentrations at defined cell densities and in the presence of sufficient concentration of blocking antibodies to reliably determine the ligand synthesis rate. Otherwise, one would obtain an incorrect ligand synthesis rate, underestimating the fraction of ligand taken up by cell receptors. This suggestion is consistent with the one previous examination of this topic for the IL-2 T-lymphocyte system (Claret et al., 1992). In that work, it was found that 25–50 nM of anti-IL-2R blocking antibody was required to permit IL-2 to escape from secreting cells at maximal levels. The IL-2 synthesis rate can be estimated under these conditions to be approximately 300 molecules/cell-minute. These findings compare favorably with our model predictions (Fig. 6) that roughly 10–100 nM of an anti-receptor blocking antibody (possessing affinity on the order of 1 nM for the receptor) would be required, blocking a sufficient fraction of

Table III. Artificially engineered cell systems.

Cell type	Plasmids	No. of clones	Induced
$EGFR^+$/TGFα	pXER/pUHD15.1/pUHD10.3-TGFα/pR9	5	1–40
EGFR–TGFα	pUHD15.1/pUHD10.3-TGFα/pR9	4	0.5–10
$EGFR^+$/EGF	pXER/pUHD15.1/pUHD10.3-EGF/pR9	2	5–200[a]
$EGFR^-$/EGF	pUHD15.1/pUHD10.3-EGF/pR9	2	2–40[a]
$EGFR^+$ mutations			
A654/EGF	pXER/pUHD15.1/pUHD10.3-EGF/pHyg.	6[b]	5–8
M721/EGF	pXER/pUHD15.1/pUHD10.3-EGF/pHyg.	12[b]	1–10
M721A654/EGF	pXER/pUHD15.1/pUHD10.3-EGF/pR9	15	1–140
Δ647/EGF	pXER/pUHD15.1/pUHD10.3-EGF/pHyg.	1	150

Note. Induction is reported as ng/million cells/24 h. [a]Will et al., 1995. [b]Not all clones tested at this time.

cell surface receptors and permitting a substantial amount of synthesized ligand to escape into the bulk extracellular medium. We note that this estimate depends on the cell density used by Clare et al.—which was not reported in their study—being sufficiently great (see Fig. 7) that cell uptake of synthesized ligand in the absence of blocking antibody is indeed significant. Such an uncertainty reiterates the need to quantify key system parameters in order to properly interpret experimental findings.

This sort of mathematical modeling approach yields important insights concerning which molecular and cellular variables and parameters govern autocrine loop behavior. With an experimentally validated model, further detailed questions can be asked regarding regulation of autocrine signaling and consequent cell responses, not only allowing more rational design of therapeutic interventions but also deeper insight into fundamental biological mechanisms. A particularly intriguing issue, for instance, is the relationship between the level of autocrine ligand found in the extracellular environment and the functional significance of an autocrine loop. More precisely, it is typically considered that autocrine signaling is most important when a large concentration of autocrine ligand is found in the bulk medium, because this condition represents a ''community effect'' signal representing cell density (e.g., Alberts et al., 1994, pp. 724–725). However, it is alternatively conceivable that the most physiologically effective autocrine regulation occurs when very little ligand escapes into the extracellular medium, and instead of reflecting information merely about cell density, the autocrine loop gives the secreting cell data about the molecular components present in its very local neighborhood; i.e., a ''sonar'' effect. Thus, it will be crucial to be able to relate measurements of extracellular autocrine ligand concentration to other key parameters of the autocrine loop to properly understand the role of a given loop in cell and tissue regulation.

We thank Manfred Gossen and Hermann Bujard for the gifts of pUHD15.1 and pUHD10.3, Rik Derynck for the TGFα vector, and Gordon Gill for the EGF receptor plasmid and the B82 mouse L cell lines. We also thank Birgit Will-Simmons for constructing the B82 cells containing pUHD15.1 and for preparation of the pR8 vector. This work was supported by a grant from the NSF Biotechnology Program, Division of Bioengineering & Environmental Systems, to D.A.L. and H.S.W.

APPENDIX

Parameter, Nomenclature, Values, and Starting Conditions

Initial Conditions

$R/R_O = 1.0$	surface receptors (all receptor initially unbound)
$C/R_O = 0.0$	surface complexes (no complexes)
$Y/R_O = 0.0$	bound receptor/antibody (no initial binding)
$B^*/B_t = 1.0$	secretion layer antibody (homogeneously distributed blocker concentration)
$B_B/B_t = 1.0$	bulk media antibody (homogeneously distributed blocker concentration)
$B_i/B_t = 1.0$	intermediate media antibody (homogeneously distributed blocker concentration)
$L^*/K_d = 0.0$	secretion layer ligand (secretion has not begun)
$L_B/K_d = 0.0$	bulk media ligand (secretion has not begun)
$L_i/K_d = 0.0$	intermediate media ligand (secretion has not begun)

K_d is the equilibrium dissociation constant and B_t is receptor blocker concentration.

Starbuck et al. (1990)

$K_d = 4.7$ nM	receptor/ligand equilibrium dissociation constant
$k_{off} = 0.34$ min^{-1}	receptor/ligand dissociation rate constant
$k_{on} = 1.2 \times 10^{-13}$ cm^3/site-min	receptor/ligand association rate constant
$k_{offa} = k_{off}$	antibody–antigen dissociation rate constant
$k_{ona} = k_{on}$	antibody–antigen association rate constant
$R_o = 100{,}000$# / cell	initial receptor number
$k_t = 0.03$ min^{-1}	constitutive internalization rate constant
$k_e = 0.3$ min^{-1}	ligand-induced internalization rate constant

Forsten et al. (1992a,b)

$k_1 = k_t$	internalization rate const., antibody/receptor
$k_2 = k_e$	induced internalization rate constant, ab/receptor/ab
$\delta = 2 \times 10^{-5}$ cm	secretion layer thickness
$\delta_{int} = 25 \times 10^{-4}$ cm	intermediate layer thickness
$a = 5 \times 10^{-4}$ cm	cell radius
$D_L = 9 \times 10^{-5}$ cm^2/min	ligand diffusion constant
$D_B = 2 \times 10^{-5}$ cm^2/min	antibody diffusion constant

Experimental Conditions

$p_{area} = 28.3\ cm^2$	60 mm dish plate area
$p_{lvol} = 5\ cm^3$	media volume
$x_{height} = pl_{vol}/p_{area}$	height of media in plate
$\Psi = p_{area}$/cell density, cm^2-cell	distance between cells, homogeneously spread
$V_b = \Psi(x_{height}-\delta_{int})$	bulk volume
$V_{cell} = 5 \times 10^{-10}\ cm^3$/cell	cell volume
$V^* = 6.5 \times 10^{-11}\ cm^3$/cell	secretion layer volume
$V_{int} = \Psi \cdot \delta_{int}-V_{cell}-V^*$	intermediate later volume
$Q = 30$–6,000#/cell-min	ligand secretion rate
$V_r = R_o/k_t$	receptor secretion rate

References

Alberts, B., Bray, D., Lewis, J., Raff, M., Roberts, K., Watson, J. D. 1994. Molecular biology of the cell. 3rd edition. Garland Press, New York.

Barnard, J. A., Graves-Deal, R., Pittelkow, M., DuBois, R., Cook, P., Ramsey, G., Bishop, P., Damstrup, L., Coffey, R. J. 1994. Auto- and cross-induction within the mammalian epidermal growth factor-related peptide family. J. Biol. Chem. **269**: 22817–22822.

Berg, H. C. 1983. Random walks in biology. 2nd edition. Princeton University Press, Princeton, N.J. pp. 30–34.

Boonstra, J., Rijken, P., Humbel, B., Cremers, F., Verkleij, A., van Bergen en Henegouwen, P. 1995. The epidermal growth factor. Cell Biol. Int. **19**: 413–430.

Carpenter, G., Wahl, M. I. 1990. The epidermal growth factor family, pp. 69–171. In: M. B. Sporn and A. B. Roberts (eds.), Peptide growth factors and their receptors. 1st edition. Springer-Verlag, New York.

Carraway, K. L., Cerione, R. A. 1993. Inhibition of epidermal growth factor receptor aggregation by an antibody directed against the epidermal growth factor receptor extracellular domain. J. Biol. Chem. **268**: 23860–23867.

Chen, W. S., Lazar, C. S., Lund, K. A., Welsh, J. B., Chang, C. P., Walton, G. M., Der, C. J., Wiley, H. S., Gill, G. N., Rosenfeld, M. G. 1989. Functional independence of the epidermal growth factor receptor from a domain required for ligand-induced internalization and calcium regulation. Cell **59**: 33–43.

Claret, E., Renversez, J. -C., Zheng, X., Bonnefoix, T., Sotto, J.-J. 1992. Valid estimation of IL-2 secretion by PHA-stimulated T-cell clones absolutely requires the use of anti-CD25 monoclonal antibody to prevent IL-2 consumption. Immunol. Lett. **33**: 179–186.

Cohen, S. 1962. Isolation of a mouse submaxillary gland protein accelerating incisor eruption and eyelid opening in the new-born animal. J. Biol. Chem. **237**: 1555–1562.

DeLarco, J. E., Todaro, G. J. 1978. Growth factors from murine sarcoma virus-transformed cells. Proc. Natl. Acad. Sci. U.S.A. **75**: 4001–4005.

Dempsey, P. J., Coffey, R. J. 1994. Basolateral targeting and efficient consumption of transforming growth factor-α when expressed in Madin-Darby canine kidney cells. J. Biol. Chem. **269**: 16878–16889.

Derynck, R., Roberts, A.B., Winkler, M.E., Chen, E.Y., Goeddel, D.V. 1984. Human transforming growth factor-α: Precursor structure and expression in E. Coli. *Cell* **38**: 287–297.

Derynck, R. 1992. The physiology of transforming growth factor-α. Adv. Cancer Res. **58**: 27–52.

Earp, H. S., Austin, K. S., Blaisdell, J., Rubin, R. A., Nelson, K. G., Lee, L. W., Grisham, J. W. 1986. EGF stimulates EGF receptor synthesis. J. Biol. Chem. **261**: 4777–4780.

Filmus, J., Trent, J. M., Pollak, M. N., Buick, R. N. 1987. Epidermal growth factor receptor gene-amplified MDA-468 breast cancer cell line and its nonamplified variants. Mol. Cell. Biol. **7**: 251–257.

Fontana, J. A., Nervi, C., Shao, Z., Jetten, A. M. 1992. Retinoid antagonism of estrogen-responsive transforming growth factor α and pS2 gene expression in breast carcinoma cells. Cancer Res. **52**: 3938–3945.

Forsten, K. E., Lauffenburger, D. A. 1992a. Autocrine ligand binding to cell receptors: Mathematical analysis of competition by solution 'decoys'. Biophys. J. **61**: 518–529.

Forsten, K. E., Lauffenburger, D. A. 1992b. Interrupting autocrine ligand-receptor binding: Comparison between receptor blockers and ligand decoys. Biophys. J. **63**: 857–861.

Forsten, K. E., Lauffenburger, D. A. 1994. The role of low-affinity interleukin-2 receptors in autocrine ligand binding: Alternative mechanisms for enhanced binding effect. Mol. Immunol. **31**: 739–751.

French, A. R., Sudlow, G. P., Wiley, H. S., Lauffenburger, D. A. 1994. Postendocytic trafficking of EGF-receptor complexes is mediated through saturable and specific endosomal interactions. J. Biol. Chem. **269**: 15749–15755.

Gill, G. N., Bertics, P. J., Santon, J. B. 1987. Epidermal growth factor and its receptor. Mol. Cell. Endocrin. **51**: 169–186.

Gong, Y., Ballejo, G., Murphy, L. C., Murphy, L. J. 1992. Differential effects of estrogen and anti-estrogen on transforming growth factor gene expression in endometrial adenocarcinoma cells. Cancer Res. **52**: 1704–1709.

Gossen, M., Bujard, H. 1992. Tight control of gene expression in mammalian cells by tetracycline-responsive promoters. Proc. Natl. Acad. Sci. U.S.A. **89**: 5547–5551.

Hamburger, A. W., Pinnamaneni, G. 1992. Interferon-induced enhancement of transforming growth factor-α expression in a human breast cancer cell line. Proc. Soc. Exp. Biol. Med. **202**: 64–68.

Knauer, D. J., Wiley, H. S., Cunningham, D. D. 1984. Relationship between epidermal growth factor receptor occupancy and mitogenic response. J. Biol. Chem. **259**: 5623–5631.

Kriegler, M. 1990. DNA transfer, pp. 96–98. 3rd edition. In: M. Kriegler, (ed.), Gene transfer and expression. W. H. Freeman and Company, New York.

Kumar, V., Cotran, R. S., Robbins, S. L. 1992. Basic Pathology, 5th edition. W. B. Saunders, Philadelphia.

Lin, C. R., Chen, W. S., Lazar, C. S., Carpenter, C. D., Gill, G. N., Evans, R. M., Rosenfeld, M. G. 1986. Protein kinase C phosphorylation at Thr 654 of the unoccupied EGF receptor and EGF binding regulate functional receptor loss in independent mechanisms. Cell **44**: 839–848.

Lund, K. A., Opresko, L. K., Starbuck, C., Walsh, B. J., Wiley, H. S., 1990. Quantitative analysis of the endocytic system involved in hormone-induced receptor internalization. J. Biol. Chem. **265**: 15713–15723.

Massague, J., Pandiella, A. 1993. Membrane-anchored growth factors. Annu. Rev. Biochem. **62**: 515–541.

Mendelsohn, J., Masui, H., Goldenberg, A. 1987. Anti-epidermal growth factor receptor monoclonal antibodies may inhibit A431 tumor cell proliferation by blocking an autocrine pathway. Trans. Assoc. Am. Physicians. **100**: 173–178.

Modjtahedi, H., Eccles, S. A., Box, G., Styles, J., Dean, C. J. 1993. Anti-tumor activity of combinations of antibodies directed against different epitopes on the extracellular domain of the human EGF receptor. Cell Biophys. **22**: 129–146.

Modjtahedi, H., Styles, J., Dean, C. 1993. The growth response of human tumor cell lines expressing the EGF receptor to treatment with EGF and/or Mabs that block ligand binding. Int. J. Oncol. **3**: 237–243.

Oehrtman, G. T., Walker, L. L., Wiley, H. S., Lauffenburger, D. A. 1997. Methods for quantitative assessment of autocrine cell loops. In: M. Yarmush and J. Morgan (eds.), Methods in tissue engineering. Humana Press, Totowa, NJ (in press).

Opresko, L. K., Chang, C. P., Will, B. H., Burke, P. M., Gill, G. N., Wiley, H. S., 1995. Endocytosis and lysosomal targeting of epidermal growth factor receptors are mediated by distinct sequences independent of the tyrosine kinase domain. J. Biol. Chem. **270**: 4325–4333.

Reiss, M., Stash, E. B., Vellucci, V. F., Zhou, Z. 1991. Activation of the autocrine transforming growth factor α pathway in human squamous carcinoma cells. Cancer Res. **51**: 6254–6262.

Rodeck, U., Williams, N., Murthy, U., Herlyn, M. 1990. Monoclonal antibody 425 inhibits growth stimulation of carcinoma cells by exogenous EGF and tumor-derived EGF/TGFα. J. Cell. Biochem. **44**: 69–79.

Sporn, M. B., Roberts, A. B. 1990. The multi-functional nature of peptide growth factors, pp. 3–15. In: Peptide growth factors and their receptors I, 1st edition. M. B. Sporn and A. B. Roberts, (eds.), Springer-Verlag, New York.

Sporn, M. B., Roberts, A. B. 1993. Autocrine secretion—10 years later. Ann. Internal Med. **117**: 408–414.

Starbuck, C., Wiley, H. S., Lauffenburger, D. A. 1990. Epidermal growth factor binding and trafficking dynamics in fibroblasts: Relationship to cell proliferation. Chem. Eng. Sci. **45**: 2367–2373.

Van der Vijver, M. J., Kumar, R., Mendelsohn, J. 1991. Ligand-induced activation of A431 cell epidermal growth factor receptors occurs primarily by an autocrine pathway that acts upon receptors on the surface rather than intracellularly. J. Biol. Chem. **266**: 7503–7508.

Wigler, M., Pellicer, A., Silverstein, S., Axel, R., Urlaub, G., Chasin, L. 1979. DNA-mediated transfer of the adenine phosphoribosyltransferase locus into mammalian cells. Proc. Natl. Acad. Sci. U.S.A. **76**: 1373–1376.

Will, B. H., Lauffenburger, D. A., Wiley, H. S. 1995. Studies on engineered autocrine systems: requirements for ligand release from cells producing an artificial growth factor. Tissue Eng. **1**: 83–96.

Yamada, Y., Serrero, G. 1988. Autocrine growth factor induced by the insulin-related factor in the insulin-dependent teratoma cell line 1246-3A. Proc. Natl. Acad. Sci. U.S.A. **85**: 5936–5940.

Zorbas, M. A., Yeoman, L. C. 1993. Growth control in a human colon carcinoma cell line mediated by cell-associated TGFα. Exp. Cell. Res. **206**: 49–57.